JOURNAL OF MATERIALS SCIENCE 21 (1986) 4206–4214

Transverse ply cracking strains in (0°/90°) and (±θ°/90°) laminates

J. G. MORLEY, G. PISSINOU
Wolfson Institute of Interfacial Technology, University of Nottingham, Nottingham, UK

Comparisons have been made between experimental data on transverse ply cracking in various types of (0°/90°) and (±θ°/90°) laminates and the predictions of the constrained cracking and strain field theory. Generally it is observed that the predictions of the strain field theory are in closer agreement with the experimental data over a wider range of experimental conditions than those of the constrained cracking model. It is shown that reasonable agreement with the observed transverse ply cracking strains of various laminates produced from similar material can be obtained through the use of a standard set of material property values.

1. Introduction

When fibre composite laminates are loaded in tension, cracks are observed to propagate parallel to the fibres in the off-axis plies. Cracking occurs at low strain values and is first observed in the transverse (90°) plies. Experimental studies of this phenomenon have been made by Bailey *et al.* [1], Crossman and Wang [2] and Flaggs and Kural [3]. Although the final fracture of a laminate is governed by fibre failure in the primary load-bearing plies, the initial cracking of the transverse and off-axis plies reduces the elastic moduli of the laminate and leads to enhanced rates of degradation by environmental attack.

A theoretical analysis of constrained cracking was given for matrix failure in fibre composites by Aveston and Kelly [4]. This was modified by Garret and Bailey [5], Bailey *et al.* [1] and Aveston and Kelly [6] to deal with laminates. This analysis has been used widely to predict the effect of the construction of a laminate on the cracking strain of transverse plies. The constrained cracking analysis is based on a calculation of the change in energy between an initial state, in which the transverse ply is uncracked, and a final state, in which a crack of infinite length exists in the transverse ply. The interply interfaces are assumed to remain intact and the amount of stress transfer across them is computed from shear lag analysis. When the laminate can be considered to be formed from a number of identical units each containing one interply interface, the transverse ply cracking strain, ε, is given by the relationship

$$\varepsilon^4 = \frac{bE_1 G_{23} G_{1c}^2}{(b + d)d^2 E_{cl} E_2^3} \quad (1)$$

where b is the thickness of the 0° (or ±θ°) plies and d is the thickness of the 90° ply, E_1 is the elastic modulus of the 0° (or ±θ°) ply, G_{23} is the transverse shear modulus of the transverse ply, G_{1c} is the work of fracture for mode 1 crack extension parallel to the fibres in the transverse ply, E_{cl} is the elastic modulus in the 0° direction of the element of laminate considered and E_2 is the elastic modulus of the transverse ply measured at right angles to the direction of fibre alignment.

Equation 1 is found to predict the experimentally observed enhanced cracking strains of transverse plies with fair accuracy when additional effects due to differential thermal contraction and Poisson effects resulting from elastic anisotropy are taken into account. The analysis is, however, only applicable for sufficiently large values of b/d where the predicted value of the transverse ply cracking strain is greater than the intrinsic cracking strain of the transverse ply.

An alternative analysis of transverse ply cracking has been proposed by Korczynskij and Morley [7]. It is based on a previous analysis of the mechanics of the growth of a crack of finite length bridged by reinforcing fibres [8, 9]. A crack of arbitrary length is assumed to propagate when the Griffith energy balance criterion is met. This was initially computed from the assumed form of the strain field surrounding a matrix crack bridged by cylindrical reinforcing members [8, 9] and has been modified to deal with a crack in a transverse ply bridged by an adjacent intact ply [7]. Experimental confirmation of the general form of the assumed strain field has now been obtained [10]. The strain field analysis has been shown previously to predict the strain for crack extension in reinforced metal sheets [9], fibre-reinforced polymers [11] and transverse ply cracking strains in cross ply laminates [7, 12]. When applied to transverse ply cracking in laminates intrinsic flaws are assumed to be present in a transverse ply and to control its failing strain when loaded independently of the other plies in the laminate. The size of the intrinsic flaws is computed on the basis of the Griffith criterion from the known properties of the transverse ply. The strain field analysis is thus capable of predicting the cracking strains of a transverse ply even when the volume fraction of intact crack bridging plies in the laminate approaches zero. Also since the analysis deals with the growth of cracks of finite size it gives some insight into possible ways by which crack growth from damaged regions may be suppressed. The strain

0022–2461/86 $03.00 + .12

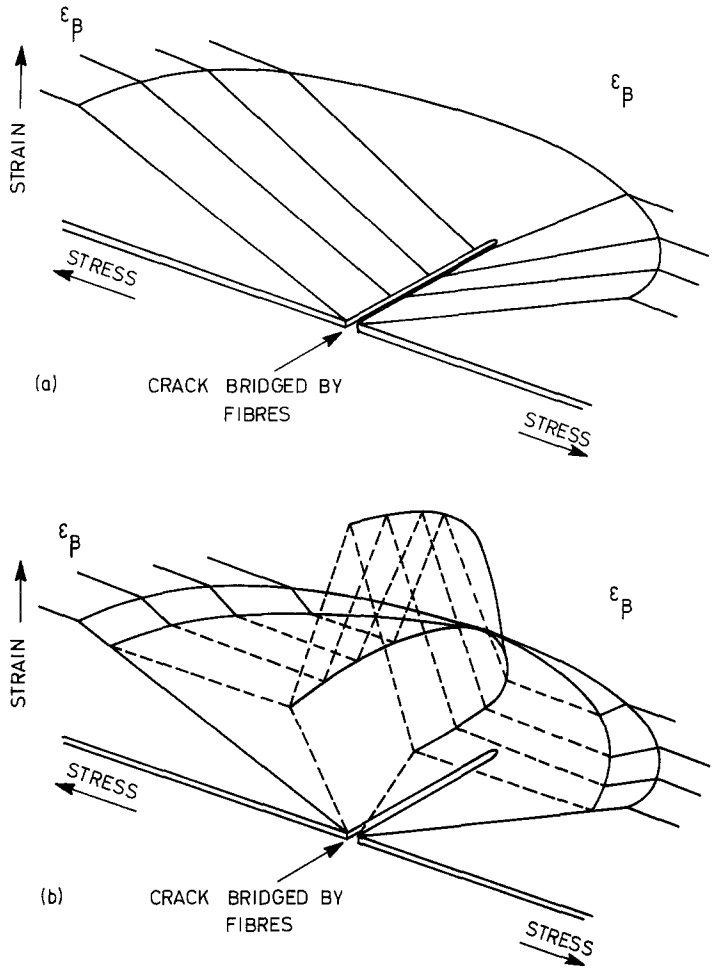

Figure 1 Assumed form of the strain field surrounding one half of a crack (a) in an unreinforced elastic sheet subjected to a uniform tensile stress acting perpendicularly to the crack faces, and (b) bridged by reinforcing members.

field analysis has also been shown to predict correctly the failing strains of unidirectional composites in which the fibres have a known distribution of strengths and the growth of damage zones in laminates [13]. It has also been shown to be consistent with the constrained cracking phenomena observed in intermingled carbon fibre glass fibre hybrid composites [14].

In this paper the predictions of the strain field model and those of the constrained cracking model are compared with experimental data on transverse ply cracking strains observed for different laminate systems by Bailey *et al.* [1], Crossman and Wang [2] and Flaggs and Kural [3].

2. Analytical procedure

The strain field model for transverse ply cracking in laminates has been described in detail elsewhere [7] and will be given only in outline here. It is based on a model previously developed to deal with the mechanics of the growth of a crack bridged by reinforcing members [8–11]. This is first briefly described and the transpositions necessary for its application to the laminate are then given.

The general form of the strain field developed around a matrix crack when no fibres are present is illustrated in Fig. 1a. Strain values are plotted vertically. The zone around the crack within which the strain field is perturbed is assumed to be elliptical in form with the crack as the minor axis of the ellipse. The major axis of the elliptical zone is three times the minor axis. Loads and strains are measured only in the loading direction and the elliptical zone is assumed to be divided into a number of parallel independent strips. The strain distribution within each strip is assumed to be zero at the crack face and to increase linearly up to ε_β, the bulk strain carried by the material, at the edge of the ellipitcal zone. On the basis of these assumptions the strain energy contained within one strip is readily calculated.

In the absence of a crack all of the strips would be carrying a uniform strain ε_β. Hence the strain energy released by the partial elastic relaxation of all of the strips in the elliptical zone due to the presence of the crack can be obtained. The size of the elliptical zone is chosen so that this is numerically equivalent to the strain energy released by an isotropic elastic material containing a crack under plane stress conditions as calculated by Griffith [15]. Thus when the fibre volume fraction is zero the strain field model predicts the same numerical value for the critical crack length as that obtained from the Griffith analysis.

The strain field shown in Fig. 1a is modified by the presence of crack bridging reinforcing fibres. Their effect is computed assuming a constant shear stress transfer value, τ, at the fibre/matrix interface. The fibres carry their maximum load where they bridge the crack and this additional load is transferred from the fibres to the matrix progressively with increasing distance from the crack face. The strain carried by the fibres therefore falls linearly with increasing distance from the crack face. The strain carried by the matrix similarly increases over its unreinforced condition. The

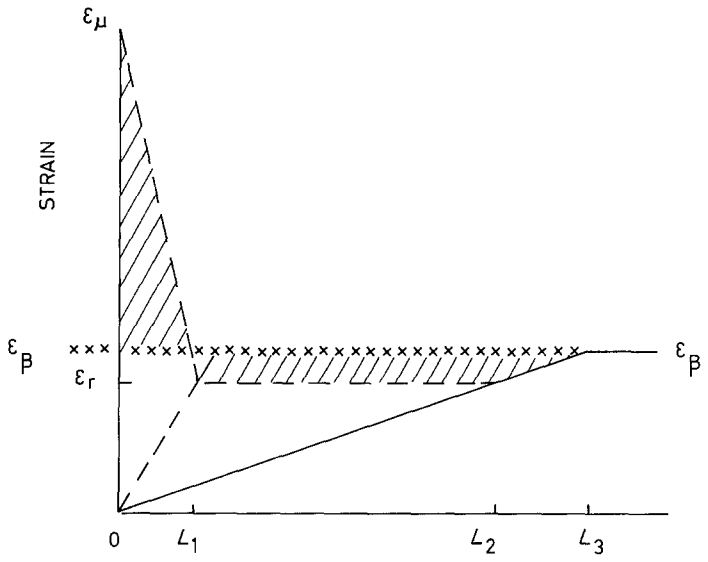

Figure 2 Strain distribution within any section of the strain field perpendicular to the crack. The diagram relates to one quadrant of the strain field, the crack being positioned at 0.

general form of the assumed strain field when crack bridging reinforcing fibres are present is illustrated in Fig. 1b.

Experimental data supporting the assumed form of the strain field have now been obtained [10]. The strain distribution between fibres and matrix within a segment of the composite parallel to the fibre alignment and loading direction is illustrated in Fig. 2. At some distance from the crack face defined as the point L_1 the strains carried by the fibres and matrix are equal and it is assumed that the strain distribution at greater distances from the crack face takes the form illustrated in Fig. 2. The relationship between the various quantities indicated in Fig. 2 are as follows:

$$\varepsilon_r = \{\varepsilon_\beta L_3/[Q(P + \varepsilon_\beta/L_3)^{-2} + L_3/\varepsilon_\beta]\}^{1/2} \quad (2a)$$

$$\varepsilon_\mu = (P + Q + \varepsilon_b/L_3) \quad (2b)$$

$$L_1 = \varepsilon_r(P + \varepsilon_\beta/L_3)^{-1} \quad (2c)$$

$$L_2 = L_3\varepsilon_r/\varepsilon_\beta \quad (2d)$$

$$L_3 = 3(a^2 - z^2)^{1/2} \quad (2e)$$

where $P = 2V_f/E_m V_m r$, $Q = 2/E_f r$. The total crack length is given by $2a$ and z is the distance of the segment considered from the centre of the crack. V_f and V_m are the fibre and matrix volume fractions and $2r$ is the fibre diameter.

The strain energy released by a strip, as defined in Fig. 2, having a width δz and unit thickness and positioned at a distance z from the centre of the crack is given by δW_{Rz} where

$$\delta W_{Rz} = \{E_c\varepsilon_\beta^2 L_3/2 - E_c\varepsilon_\beta^2(L_3^3 - L_2^3)/6L_3^2 - E_c\varepsilon_r^2(L_2 - L_1)/2 - E_m V_m \varepsilon_r^2 L_1/6 - V_f E_f(\varepsilon_\mu^2 + \varepsilon_\mu\varepsilon_r + \varepsilon_r^3)L_1/6\}\,\delta z \quad (3)$$

E_f and E_m are the Young's modulus values of fibres and matrix, respectively, and the other symbols have their usual meanings. The strain energy released by the material within the whole of the elliptical zone can be obtained by numerical integration. The rate of release of strain energy with increasing crack length can then be obtained by numerical differentiation.

Strain energy is absorbed in rupturing the matrix and for the purposes of calculation a transverse planar crack is assumed to be present. Energy is also absorbed in rupturing the chemical bond between the fibres and the matrix and by frictional losses developed by differential movement between the crack bridging fibres and the matrix. The energy absorbed by frictional losses within a segment of the ellipse width δz and of unit thickness is given by:

$$\delta W_{Az} = V_f\tau\varepsilon_\mu L_1^2\delta z/3r \quad (4)$$

If the work done in debonding a unit area of fibre matrix interface is G_d the work done, W_d, on each side of the crack per unit increase in crack area will be given by:

$$W_d = 4V_f L_1 G_d/r \quad (5)$$

The presence of crack bridging fibres reduces the rate of release of strain energy with the increasing length of a matrix crack compared with an unreinforced material. Also the rate of absorption of energy increases with increasing crack length because of the additional crack length dependent energy absorbing processes discussed above. Hence the stability of a matrix crack is enhanced considerably by the presence of the fibres.

The model described above can be modified to deal with crack propagation in the transverse plies of a laminate [7]. The 0° or $\pm\theta$° plies remain intact and bridge the crack in the transverse ply (Fig. 3). Load is transferred between the longitudinal and transverse plies across the interply interface. This is assumed to take place at a constant shear stress value τ. The laminate can be assumed to be formed from a number of identical cells each containing part of a longitudinal and transverse ply and one interply interface. The thickness of the longitudinal ply (0° or $\pm\theta$°) is termed T_l and the tranverse ply thickness is termed T_t. The total thickness of the two ply laminate illustrated in Fig. 3 is termed T_{tot}.

In order to transpose Equations 2, 3, 4 and 5 from a fibre matrix system to a two-ply unit cell laminate the following substitutions are made: T_l for V_f, T_t for V_m, E_l for E_f, E_t for E_m and $1/T_l T_{tot}$ for $2/r$. The elastic modulus of the laminate in the direction of loading is substituted for E_c. It can be calculated using laminae

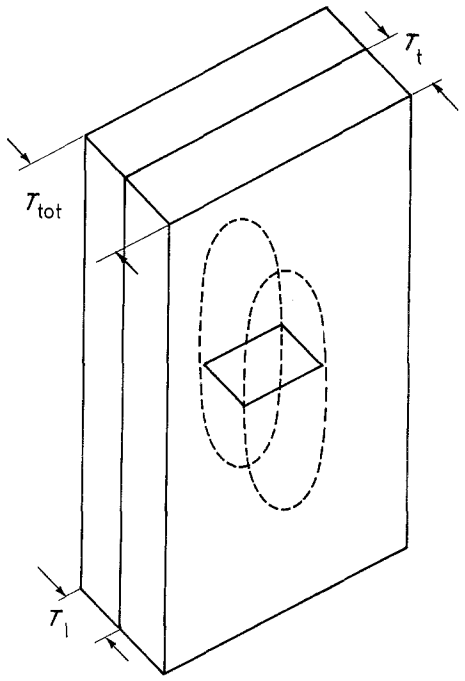

Figure 3 Illustration of a through crack in the transverse ply of a laminate "unit cell".

elasticity theory. The computation of the critical strains for crack extension is thus obtained from a consideration of the fibre system which is equivalent to the laminate and is obtained by the above transpositions. The fracture analysis takes into account chemical debonding of the fibre/matrix interface and when applied to laminates the analysis refers to interply debonding. Where interply debonding does not occur energy is not absorbed by this process and the parameter G_d is set to zero for these conditions. The fibre analysis also refers to frictional losses incurred by differential movement between fibres and matrix against a constant frictional loss term, τ. Energy losses of this type have been retained in the laminate analysis since differential movement between the plies is assumed to occur. Energy is assumed to be dissipated by elastic–plastic deformation of the polymeric material at the interply interface, by reason of the shear stress, τ, developed there.

The analysis of crack growth in the transverse plies in a laminate developed here should be regarded only as approximate since various simplifying assumptions are made. For example, a full account is not taken of the elastic anisotropy of the laminae. Also the shear stress transfer across the interply interface is assumed to take place at a constant rate, τ, instead of the non-uniform rate to be expected from elastic shear lag analysis. A more complex model would be required in order to overcome these limitations. The present approximate analysis has been found previously to predict the cracking strains of transverse plies in 0°/90° laminates quite accurately [7, 11].

3. Preliminary considerations

3.1. Intrinsic crack sizes

The transverse ply cracking strains computed from the strain field analysis are the laminate strains at which intrinsic flaws or cracks present in the transverse ply become unstable. The intrinsic crack sizes have been estimated from the Griffith equation:

$$a = G_c/\pi\varepsilon_{fr}^2 E \quad (6)$$

where a is the length of an edge crack and $2s$ the length of a central crack, ε_{fr} is the strain for unstable crack growth, E is the Young's modulus for the transverse ply measured perpendicularly to the direction of fibre alignment (i.e. E_2) and G_c is the work of fracture within the body of the transverse ply. Bailey *et al.* [1] give limits for their experimental values of G_c, ε_{fr} and E_t. These limits can be combined in the Griffith equation in eight possible ways giving eight possible limiting values for the half-crack length a. These range from 0.15 to 0.417 mm.

3.2. Interlaminar shear stress transfer rates

In order to compute the transverse ply cracking strains from the strain field analysis it is necessary to obtain a value for τ the interlaminar shear stress transfer rate. For the approximate computation presented here it is assumed to have a constant value over the distance from 0 to L_1 in Fig. 2. We have calculated the stress transfer rate from shear lag considerations as described by Garrett and Bailey [5]. From the shear lag analysis the value of τ changes progressively with increasing distances from the crack face and the numerical values are different for the different systems considered.

A value of τ of 10 MPa had been used in previous computations [7] and preliminary calculations were carried out using the strain field analysis with this value for τ. The computed values of L_1 were found to vary from very small values up to about 0.5 mm for the various crack sizes and laminate systems considered. The stress transfer rate was computed, using shear lag analysis, at the position of the crack face and at a distance of 0.5 mm from the crack face for the various systems considered. The effective values of τ obtained were 24.6 and 4.5 MPa for the $(0_2^\circ/90_1^\circ)_s$ system [1]; 27.5 and 21.6 MPa for the $(0_2^\circ/90_8^\circ)_s$ system [3]; and 33.7 and 10.5 MPa for the $(\pm 30^\circ/90_2^\circ)_s$ system [3]. It was therefore decided to compute transverse ply cracking strains for all systems studied using two fixed values of τ, i.e. 10 and 20 MPa. These were felt to be representative of the stress transfer rates likely to be encountered and the procedure enabled the effect of changes in τ to be identified.

3.3. Laminate elastic modulus values

Both the constrained cracking theory and the strain field analysis require the evaluation of the elastic modulus of the laminate in the direction of loading. For some systems this can be obtained with reasonable accuracy using a simple rule of mixtures approach. More accurate values can be obtained using laminate theory and we have used this procedure in calculating the laminate elastic moudlus values. Values calculated using laminate theory from experimental data for the individual laminae given by Bailey *et al.* [1], Flaggs and Kural [3], Crossman and Wang [2] are used in Sections 4.1, 4.2 and 4.3, respectively. These were found to agree closely with the reported experimental values of the laminate elastic properties.

TABLE I

E_1	=	$142.77 \times 10^9 \text{N m}^{-2}$
E_2	=	$10.64 \times 10^9 \text{N m}^{-2}$
ν_{12}	=	0.293
G_{12}	=	$5.5 \times 10^9 \text{N m}^{-2}$
G_{23}	=	$3.2 \times 10^9 \text{N m}^{-2}$
G_c	=	203.1J m^{-2}
ε_{fr}	=	0.00409
a	=	0.36 mm

Since the experimental values of laminae elastic properties given by the various investigators were quite similar, an average set of values for the elastic properties of a lamina was then computed from the experimental data. These are shown in Table I. Using these average values, transverse ply cracking strains were calculated. In Section 4.4 these are compared with the experimental cracking strain values given by Bailey *et al.* [1], Flaggs and Kural [3] and Crossman and Wang [2].

4. Results of calculations

In this section, calculated transverse ply cracking strains for carbon fibre epoxy resin laminates are compared with experimental values given by Bailey *et al.* [1], Flaggs and Kural [3] and Crossman and Wang [2]. The cracking strains have been calculated using both the constrained cracking theory for laminates (Bailey *et al.* [1]) and the strain field theory proposed for laminates by Korczynskij and Morley [7]. The strain field model has provision for including the energy absorbed during debonding of the interply interface. Since debonding was not observed in the systems studied, this energy loss parameter was set to zero in the calculations.

4.1. Results for carbon fibre epoxy resin cross plied systems investigated by Bailey *et al.* [1]

As indicated in Section 3.1, the range of mechanical properties given for this system resulted in eight possible lengths for the intrinsic flaw size. Each flaw size corresponded to a particular combination of transverse elastic modulus, E_2, cracking strain value, ε_{fr}, and work of fracture, G_c. These parameters were used in the strain field analysis to obtain a range of predicted cracking strains for the transverse ply in the laminate. Owing to the influence of the other physical parameters on the cracking strain values the upper and lower bounds for the cracking strains do not correspond with the maximum and minimum crack length values but to half crack lengths of 0.275 and 0.282 mm. The upper and lower limits of transverse ply cracking strain values calculated in this way for τ values of 10 and 20 MPa are shown in Figs 4 and 5. Also shown are the experimental observations of Bailey *et al.* [1], corrected for differential thermal contraction effects, and the transverse ply cracking strain values computed from the constrained cracking theory. The relatively wide range between the computed upper and lower bounds illustrate the effects which might be expected from the variability in the experimental data noted by Bailey *et al.* [1]. From Fig. 4 it can be seen that all of the experimental observations for 0°/90°/0° laminates fall within the envelope of cracking strain values computed for τ values of 10 MPa. For the 90°/0°/90° laminates shown in Fig. 5 they all fall within the envelope of cracking strain values computed for τ values of 20 MPa. It should be noted that the strain field model has been shown to predict cracking strain values very close to the experimental observations for both experimental systems when a half-crack length of 0.22 mm and a τ value of 10 MPa were used in the computation.

In the comparison between theory and experimental data which follows, mean mechanical property values have been used in the computations.

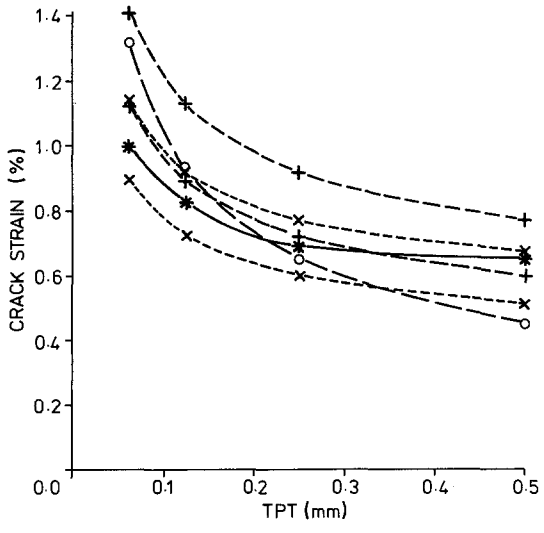

Figure 4 0°/90°/0° laminate. Thickness of 0° plies is constant at 0.5 mm. Transverse (90°) ply cracking strain shown against transverse ply thickness, TPT. (*) Experimental data from [1]; maximum and minimum cracking strains computed from strain field model with (×) τ = 10 MPa and with (+) τ = 20 MPa. (○) Computed values from constrained cracking model [1].

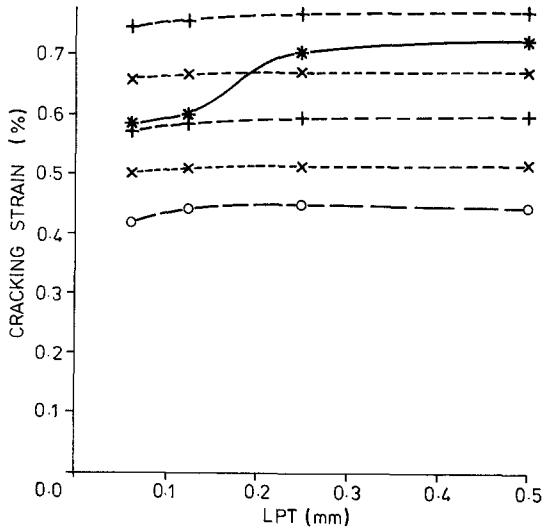

Figure 5 90°/0°/90° laminate. Thickness of 90° plies constant at 0.5 mm. Transverse (90°) ply cracking strain shown plotted against longitudinal (0°) ply thickness (LPT). Maximum and minimum cracking strains computed from strain field model with (×) τ = 10 MPa and with (+) τ = 20 MPa. (○) Computed values from constrained cracking model [1]. (*) Experimental values from [1].

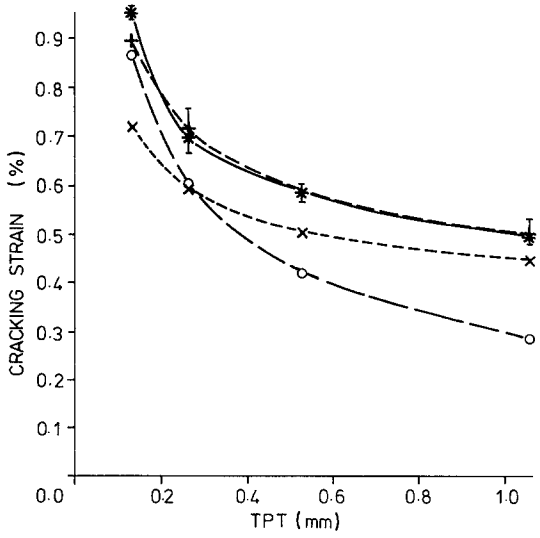

Figure 6 $(0_2/90_n^\circ)_s$ laminate. Transverse ply cracking strain plotted against thickness of transverse (90°) plies (TPT) calculated on unit cell basis (see Fig. 3). Cracking strains computed from strain field model with (×) τ = 10 MPa strain and with (+) τ = 20 MPa. (○) Computed values from constrained cracking model [1]. (*) Experimental values from [3] with error bars indicated.

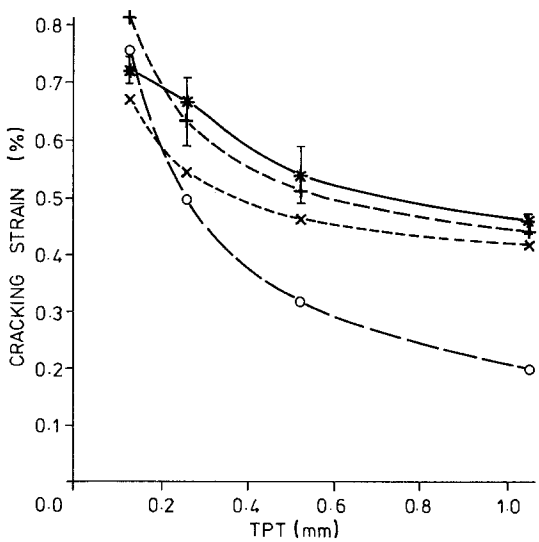

Figure 8 $(\pm 60^\circ/90_n^\circ)_s$ laminate. Transverse ply cracking strain plotted against thickness of transverse (90°) plies (TPT) calculated on unit cell basis (see Fig. 3). Cracking strains computed from strain field model with (×) τ = 10 MPa and with (+) τ = 20 MPa. (○) Computed values from constrained cracking model [1]. (*) Experimental values from [3] with error bars indicated.

4.2. Results for $(0_2^\circ/90_n^\circ)_s$ $(\pm 30^\circ/90_n^\circ)_s$ and $(\pm 60^\circ/90_n^\circ)_s$ carbon fibre epoxy resin laminates investigated by Flaggs and Kural [3]

Experimental cracking strain values obtained by Flaggs and Kural [3] for the above systems are shown in Figs 6 to 8. The error bars indicate the range of experimental values quoted by these authors. For this system a half-crack length of 0.437 mm is obtained for the intrinsic flaw size when the published lamina property values are inserted into the Griffith equation. The elastic modulus of the $\pm\theta^\circ$ plies in the loading direction was computed from laminate theory. These values were used together with the experimentally observed transverse elastic modulus E_t and work of fracture G_c to calculate the transverse ply cracking strain using the strain field theory. Values of τ of 10 and 20 MPa are assumed. Transverse ply cracking strain values were also computed using the constrained cracking theory of Bailey *et al.* These computed values are also shown in Figs 6 to 8.

Both analytical models predict cracking strain values close to the observed values when the total laminate thickness is small. This corresponds to relatively small thicknesses for the transverse ply and hence a significantly enhanced value for its cracking strain. The predictions of the strain field model are closer to the experimental observations than those of the constrained cracking theory at larger total laminate thicknesses which correspond to larger transverse ply relative thicknesses. The limitations of the constrained cracking model are apparent under these conditions since the cracking strain value of the transverse ply is predicted to approach zero as the relative thickness of the crack bridging longitudinal ($\pm\theta^\circ$) ply becomes very small.

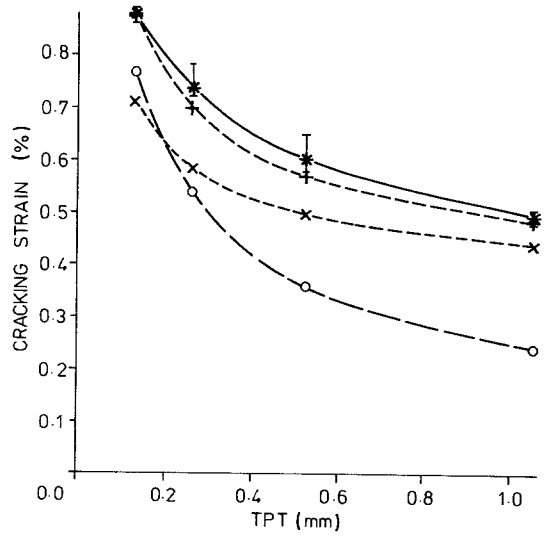

Figure 7 $(\pm 30^\circ/90_n^\circ)_s$ laminate. Transverse ply cracking strain plotted against thickness of transverse (90°) plies (TPT) calculated on unit cell basis (see Fig. 3). Cracking strains computed from strain field model with (×) τ = 10 MPa and with (+) τ = 20 MPa. (○) Computed values from constrained cracking model [1]. (*) Experimental values from [3] with error bars indicated.

4.3. Results for $(\pm 25^\circ/90_n^\circ)_s$ carbon fibre epoxy resin lamiante investigated by Crossman and Wang [2]

Crossman and Wang [2] studied the onset of interply debonding and transverse ply cracking in $(\pm 25^\circ/90_n^\circ)_s$ carbon fibre epoxy resin laminates. We have extracted the experimental values for the cases where transverse cracking occurred before delamination. We have corrected the cracking strains reported by Crossman and Wang for thermal stresses produced by differential thermal contraction using values interpolated from Flaggs and Kural's data [3] relating to $(\pm 60^\circ/90_n^\circ)_s$ and $(\pm 30^\circ/90_n^\circ)_s$ systems. The experimental material used in both studies was similar but the thermal correction value obtained should be regarded only as approximate. The experimental transverse ply cracking values obtained by Crossman and Wang and corrected

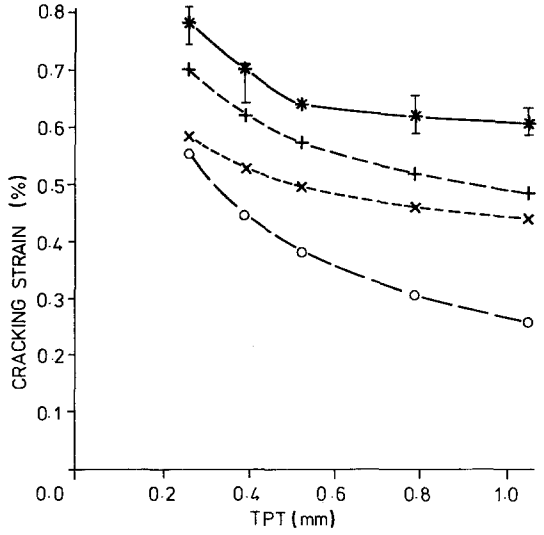

Figure 9 ($\pm 25°/90°_n)_s$ laminate. Transverse ply cracking strain plotted against thickness of transverse (90°) plies (TPT) calculated on unit cell basis (see Fig. 3). Cracking strains computed from strain field model with (×) τ = 10 MPa and with (+) τ = 20 MPa. (○) Computed values from constrained cracking model [1]. (*) Experimental values from [2] with error bars indicated.

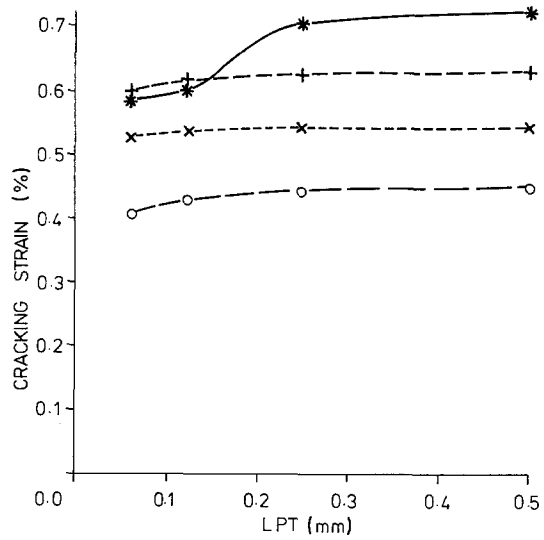

Figure 11 (90°/0°/90°) laminate. Thickness of 90° plies constant at 0.5 mm. Transverse (90°) ply cracking strain shown plotted against longitudinal (0°) ply thickness (LPT). (*) Experimental data from [1]. Computed cracking strain values from strain field model using average laminae properties (Table I) (×) for τ = 10 MPa and (+) for τ = 20 MPa. (○) Computed values from constrained cracking model [1] using average laminae properties (Table I).

in this way are shown plotted as a function of total ply thickness in Fig. 9 with the range of experimental limits quoted by the authors indicated.

A half-crack length of 0.44 mm was computed for the size of the intrinsic flaws in the transverse ply in this system using the quoted material properties. The transverse ply cracking strains were computed from the strain field model using the same procedure as that described in Section 4.2. These results are plotted in Fig. 9 for τ values of 10 and 20 MPa. The agreement between the experimental values and the predictions of the analytical model is not so good as it was with the previous systems studied and part of this discrepancy may be due to the procedure used to obtain the thermal strain correction. It will be noted that the constrained cracking model gives values which differ from the experimental values by even greater amounts.

4.4. Correlation between the various systems studied

The materials used by Flaggs and Kural and by Crossman and Wang were nominally identical carbon fibre epoxy resin systems (T300/934). Very similar material was also used by Bailey *et al.* It was thus of interest to compare the experimental observed cracking strains with the values predicted by the various analyses using a single set of data for the material properties. Average material property values were obtained from those given by the various authors and used to calculate

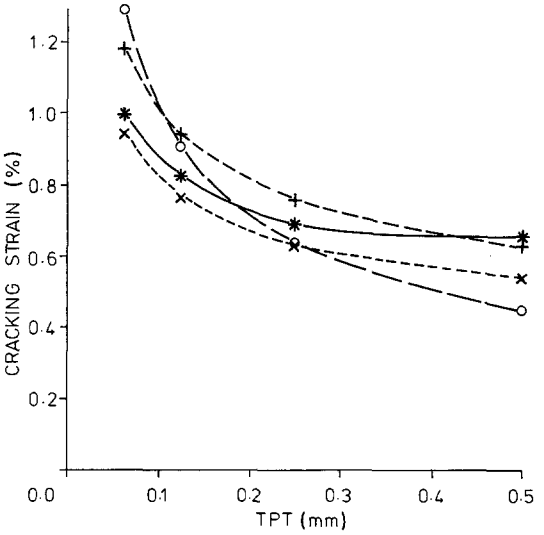

Figure 10 (0°/90°/0°) laminate. Thickness of 0° plies constant at 0.5 mm. Transverse (90°) ply cracking strain shown against transverse ply thickness (TPT). (*) Experimental data from [1]. Computed cracking strain values from strain field model using average laminae properties (Table I) (×) for τ = 10 MPa and (+) for τ = 20 MPa. (○) Computed values from constrained cracking model [1] using average laminae properties (Table I).

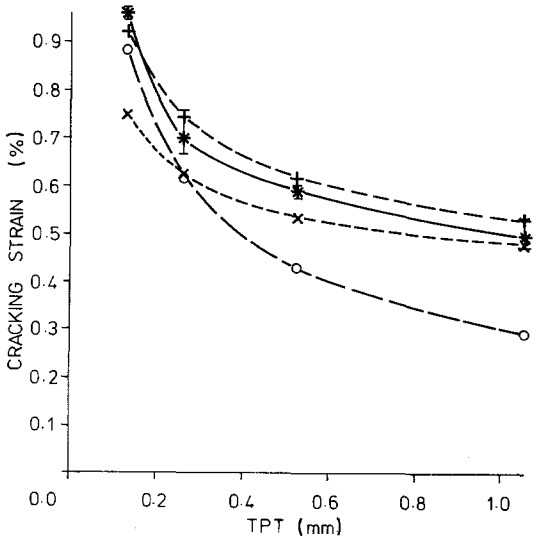

Figure 12 $(0°/90°_n)_s$ laminate. Transverse ply cracking strain plotted against thickness of transverse (90°) plies (TPT) calculated on unit cell basis (see Fig. 3). Computed cracking strain values from strain field model using average laminae properties (Table I) (×) for τ = 10 MPa and (+) for τ = 20 MPa. (○) Computed values from constrained cracking model [1] using average laminae properties (Table I). (*) Experimental data from [3] with error bars indicated.

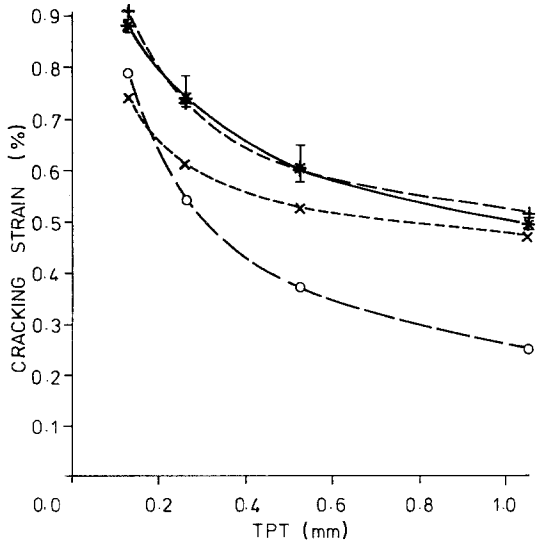

Figure 13 $(\pm 30°/90°_n)_s$ laminate. Transverse ply cracking strain plotted against thickness of (90°) plies (TPT) calculated on unit cell basis (see Fig. 3). Computed cracking strain values from strain field model using average laminae properties (Table I) (×) for τ = 10 MPa and (+) for τ = 20 MPa. (○) Computed values from constrained cracking model [1] using average laminae properties (Table I). (*) Experimental data from [3] with error bars indicated.

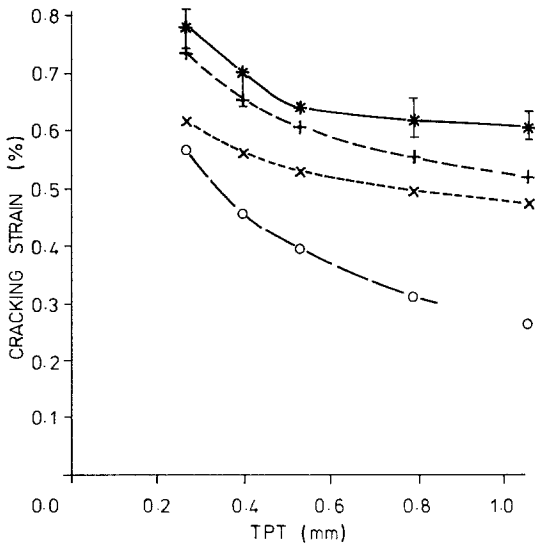

Figure 15 $(\pm 25°/90°_n)_s$ laminate. Transverse ply cracking strain plotted against thickness of transverse (90°) plies (TPT) calculated on unit cell basis (see Fig. 3). Cracking cracking strain values from strain field model using average laminae properties (Table I) (×) for τ = 10 MPa and (+) for τ = 20 MPa. (○) Computed values from constrained cracking model [1] using average laminae properties (Table I). (*) Experimental data from [2] with error bars indicated.

the appropriate cracking strains for the strain field model (see Table I). A half-crack length value of 0.36 mm was used. Similarly transverse ply cracking strains were computed using the constrained cracking model. The results of these calculations are compared with the experimental data of Bailey *et al.* [1] for the (0°/90°/0°) system and the (90°/0°/90°) system in Figs 10 and 11. Previous calculations [12] have indicated little difference in the cracking strains of the transverse plies in a 90°/0°/90° three-ply laminate whether a crack extends in one or both of the 90° plies. This effect is due to the limited constraint provided by one intact 90° ply to crack extension in the other.

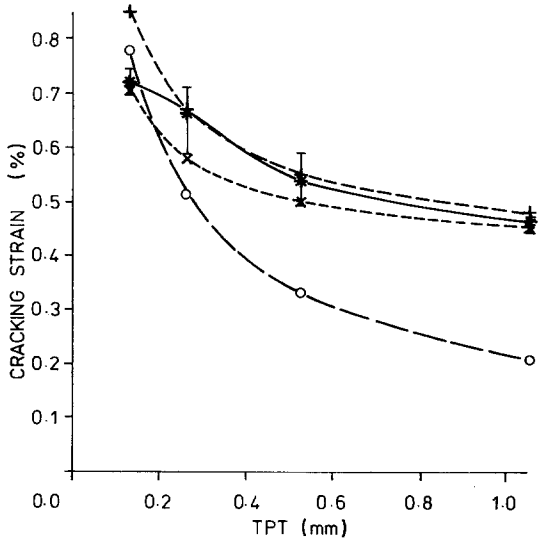

Figure 14 $(\pm 60°/90°_n)_s$ laminate. Transverse ply cracking strain plotted against thickness of transverse (90°) plies (TPT) calculated on unit cell basis (see Fig. 3). Cracking strains computed from strain field model using average laminae properties (Table I) with (×) τ = 10 MPa and with (+) τ = 20 MPa. (○) Computed values from constrained cracking model [1] using average laminae properties (Table I). (*) Experimental data from [3] with error bars indicated.

Similar comparisons are made in Figs 12 to 14 with the data given by Flaggs and Kural [3] for the $(0°_2/90°_n)_s$ system, the $(\pm 30°/90°_n)_s$ system, and the $(\pm 60°/90°_n)_s$ system. A comparison with the data of Crossman and Wang [2] for the $(\pm 25°/90°_n)_s$ system is shown in Fig. 15. These results show that reasonable agreement is obtained between the predictions of the strain field model (for a value of 20 MPa for τ) and all of the experimental observations using a single set of material properties. The constrained cracking model also predicts cracking strain values close to the experimental values for all systems providing the relative thickness of the transverse ply is small (small value of T_{tot}). The predictions of this model, however, differ increasingly from the experimental observations as the relative thickness of the transverse ply increases.

5. Conclusions

The calculations reported above show that both the constrained cracking model [1] and the strain field model [7] are capable of predicting the cracking strains of a transverse ply in a laminate with reasonable accuracy. The predictions of the strain field model are, however, applicable over a wider range of laminate geometries than those of the constrained cracking model. Reasonable agreement with available experimental data, relating to various types of laminates constructed from nominally similar material, can be obtained from the strain field model using average material property values.

Acknowledgements

The work reported here was carried out with the support of the Science and Engineering Research Council and Dunlop Ltd.

References

1. J. E. BAILEY, P. T. CURTIS and A. PARVIZI, *Proc. Roy. Soc. Lond.* **A366** (1979) 599.

2. F. W. CROSSMAN and A. S. D. WANG, The dependence of transverse cracking and delamination on ply thickness in graphite/epoxy laminates in "Damage in Composite Materials", edited by K. L. Reifsnider, ASTM, STP775 (American Society for Testing and Materials, Philadelphia, Pennsylvania, 1982) p. 118.
3. D. L. FLAGGS and M. H. KURAL, *J. Compos. Mater.* **16** (1982) 103.
4. J. AVESTON and A. KELLY, *J. Mater. Sci.* **8** (1973) 352.
5. K. W. GARRATT and J. E. BAILEY, *ibid.* **12** (1977) 157.
6. J. AVESTON and A. KELLY, *Phil. Trans. Roy. Soc. Lond.* **A294** (1980) 519.
7. Y. KORCZYNSKYJ and J. G. MORLEY, *J. Mater. Sci.* **16** (1981) 1785.
8. J. G. MORLEY and I. R. McCOLL, *J. Phys. D. Appl. Phys.* **8** (1975) 15.
9. I. R. McCOLL and J. G. MORLEY, *Phil. Trans. Roy. Soc.* **287** (1977) 17.
10. J. G. MORLEY and I. R. McCOLL, *J. Mater. Sci.* **19** (1984) 3407.
11. I. R. McCOLL and J. G. MORLEY, *ibid.* **12** (1977) 1165.
12. J. G. MORLEY, *ibid.* **18** (1983) 1564.
13. *Idem, ibid.* **20** (1985) 1794.
14. *Idem, ibid.* **20** (1985) 3939.
15. A. A. GRIFFITH, *Phil. Trans. Roy. Soc.* **A221** (1920) 163.

Received 9 January
and accepted 13 March 1986